BIOCHEMISTRY
including biophysical chemistry & molecular biology

ARTICLE

pubs.acs.org/biochemistry

Aptamer-Mediated Inhibition of *Mycobacterium tuberculosis* Polyphosphate Kinase 2

Ka To Shum,[†] Eric Lik Hang Lui,[†] Sybil Cheuk Ki Wong,[†] Pok Yeung,[†] Laiju Sam,[†] Ying Wang,[‡] Rory M. Watt,[*,‡] and Julian A. Tanner[*,†]

[†]Department of Biochemistry, Li Ka Shing Faculty of Medicine, and [‡]Oral Biosciences, Faculty of Dentistry, The University of Hong Kong, Pokfulam, Hong Kong, China

Supporting Information

ABSTRACT: Inorganic polyphosphate (polyP) plays a number of critical roles in bacterial persistence, stress, and virulence. PolyP intracellular metabolism is regulated by the polyphosphate kinase (PPK) protein families, and inhibition of PPK activity is a potential approach to disrupting polyP-dependent processes in pathogenic organisms. Here, we biochemically characterized *Mycobacterium tuberculosis* (MTB) PPK2 and developed DNA-based aptamers that inhibit the enzyme's catalytic activities. MTB PPK2 catalyzed polyP-dependent phosphorylation of ADP to ATP at a rate 838 times higher than the rate of polyP synthesis. Gel filtration chromatography suggested MTB PPK2 to be an octamer. DNA aptamers were isolated against MTB PPK2. Circular dichroism revealed that aptamers grouped into two distinct classes of secondary structure; G-quadruplex and non-G-quadruplex. A selected G-quadruplex aptamer was highly selective for binding to MTB PPK2 with a dissociation constant of 870 nM as determined by isothermal titration calorimetry. The binding between MTB PPK2 and the aptamer was exothermic yet primarily driven by entropy. This G-quadruplex aptamer inhibited MTB PPK2 with an IC_{50} of 40 nM and exhibited noncompetitive inhibition kinetics. Mutational mechanistic analysis revealed an aptamer G-quadruplex motif is critical for enzyme inhibition. The aptamer was also tested against *Vibrio cholerae* PPK2, where it showed an IC_{50} of 105 nM and insignificant inhibition against more distantly related *Laribacter hongkongensis* PPK2.

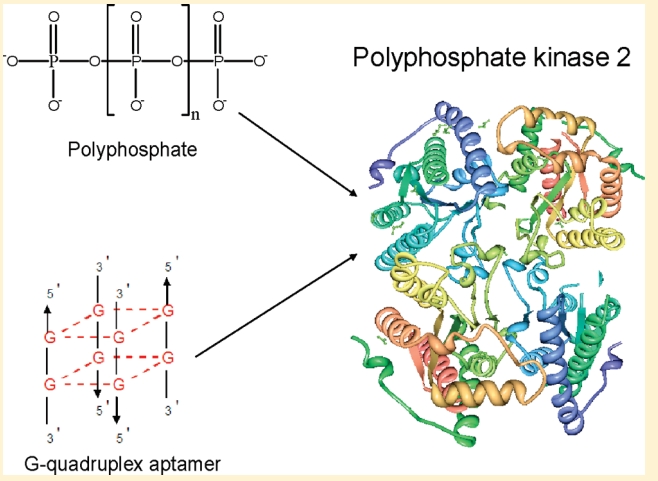

The increasing prevalence of multidrug-resistant tuberculosis (MDR-TB) is a significant world health problem. While drugs such as isoniazid and rifampicin have been historically successful in the treatment of TB caused by infection with the high-GC content Gram-positive bacterium *Mycobacterium tuberculosis*, more effective methods of combatting MDR-TB are critically required.[1] Inorganic polyphosphates (polyP) have been implicated in bacterial survival and stress response,[2] and the polyP metabolic pathways are potential therapeutic targets for chemotherapy, which has recently been highlighted particularly for mycobacteria.[3−5]

Inorganic polyphosphates (polyP) comprise tens to hundreds of phosphate residues linked linearly by phosphoanhydride bonds and have been observed to be present in every cell in nature.[6] In prokaryotes, the molecule plays a critical role in physiological adjustments to growth, development, stress, and nutrient deprivation.[7,8] In eukaryotes, the molecule has recently been shown to be a regulatory factor in proliferative signaling pathways of mammalian cells and in blood coagulation.[9−11] It is clear that this "simple" inorganic molecule plays fundamental and crucial roles that are only just beginning to be unraveled. PolyP has long been regarded as a storage form of phosphate and energy in mycobacteria, accumulating during the stationary period and utilized during active growth, with polyphosphate deficiency leading to structural and functional defects.[12−14] Enzymes have been observed in mycobacteria for both synthesis and utilization of polyP,[15] and how polyphosphate inhibits class III adenylate cyclases in *Mycobacterium bovis* as a component of the mycobacterial stress response has recently been described.[16] In addition, polyP has been shown to be intimately involved in mycobacterial persistence in the stationary phase, stress response, and virulence, implying that the polyphosphate kinases (PPKs), the major enzymes of polyP metabolism, are potential targets for antibacterials against tuberculosis.[17−19]

Received: May 20, 2010
Revised: March 7, 2011
Published: March 07, 2011

M. tuberculosis has two separate classes of polyphosphate kinases, PPK1 and PPK2.[20] *M. tuberculosis* PPK1 was recently biochemically characterized and observed to synthesize polyP using ATP. Knockout of *ppk1* resulted in the inability of *M. tuberculosis* to survive under long-term hypoxia,[17,18] and vulnerability in antisense knockdown recently showed PPK1 to be a suitable drug target.[5] With regard to PPK2, the enzyme has been characterized in *Pseudomonas aeruginosa*, *Corynebacterium glutamicum*, *Campylobacter jejuni*, and recently *M. tuberculosis*.[4,21−23] The main role of PPK2 is likely to recover energy from polyphosphate to catalyze the synthesis of NTP from NDP. *M. tuberculosis* PPK2 was expressed in the exponential phase of growth and remained at a steady level in the stationary phase in *M. tuberculosis*.[4] The protein exhibited polyP catabolic activity to generate energy rich nucleotides that is likely critical in the recovery from the stationary phase and may contribute to cell wall synthesis.[4,22] In addition, a PPK2 crystal structure has been determined recently.[24] Downregulation of PPK2 in cells compromised the ability of mycobacteria to withstand thermal and acid stress as well as hypoxia and inhibited the ability of *M. tuberculosis* to multiply in macrophages.[4] Such recent data for the critical role of PPK2 suggest that in addition to PPK1, PPK2 is another promising target for therapy.[4,25,26] However, to date, no reports of inhibitors against any polyphosphate-metabolizing enzymes have appeared.

Systematic evolution of ligands by exponential enrichment (SELEX) is an approach to screening nucleic acid libraries to identify molecules that bind and potentially inhibit a target with high affinity and selectivity.[27] There are a number of parallels with antibody technology, but nucleic acid aptamers hold several advantages for therapeutics and molecular recognition.[28] The greatest success to date is Macugen, the first FDA-approved aptamer drug for human use, for the treatment of age-related macular degeneration.[29] Because of their tight and selective binding, aptamers also have various diagnostic and biotechnological applications.[30,31] Given recent developments in the delivery of nucleic acids to *M. tuberculosis*, nucleic acid-based inhibitors may be a potential approach to inhibiting *M. tuberculosis*.[32,33]

In this study, we cloned, expressed, and purified *M. tuberculosis* PPK2 in a recombinant form and characterized its biochemical properties. We found that *M. tuberculosis* PPK2 is a polyphosphate-dependent nucleoside diphosphate kinase, which forms a stable octameric multimer. We then selected and developed inhibitory DNA aptamers against MTB PPK2. Two families of aptamers were identified, but only G-quadruplex aptamers effectively bound and inhibited PPK2. We also provide a mechanistic basis for the observed inhibition by enzyme kinetics, mutation, and truncation studies.

MATERIALS AND METHODS

Source of Genomic DNA and Cloning. The genomic DNA of the *M. tuberculosis* H37Rv strain was kindly provided by W. C. Yam (Department of Microbiology, Li Ka Shing Faculty of Medicine, The University of Hong Kong). The *ppk2* gene was amplified from the genomic DNA by polymerase chain reaction (PCR) with the forward primer (5′-GTAGGATCCATGGATATACCATCCGTTGA-3′) and the reverse primer (5′-GTAGCGGCCGCTCACCGGGCGATCAACGT-3′). The PCR product was gel purified, digested with BamHI and NotI, and ligated with a similarly digested pET32a(+) vector (Novagen) to produce plasmid pET32a-PPK2. The *ppk2* (LHK_00958) gene from *Laribacter hongkongensis* (strain HLHK9, generously provided by P. Woo, Department of Microbiology, Li Ka Shing Faculty of Medicine, The University of Hong Kong) was amplified using the LHKppk2F (5′-ATATCCATGGGTAGTGAAAACGGCATCAGCC-3′) and LHKppk2R (5′-TTAACTCGAGTTAAAGCTTGAATACCTGGGATACGTCCATTATC-3′) primers and cloned into a pET28a(+) vector (Novagen) via NcoI and XhoI. The *ppk2* (VC0728) gene from *Vibrio cholerae* 01 (El Tor biotype, strain Bah-2; generously provided by M. Waldor, Harvard University, Cambridge, MA) was amplified using the VC0728for1 (5′-ATATGGATCCCATATGGCGAAATTGGATAAGAAAGTC-3′) and VC0728rev1 (5′-TTAAGCGGCCGCTTAAAGCTTTTAGTAGCGCTGTGGAACAAAGG-3′) primers and cloned into a pET28a(+) vector (Novagen) via BamHI and XhoI.

Expression and Purification of *M. tuberculosis* PPK2. Two liters of LB broth supplemented with ampicillin (50 μg/mL) was inoculated (1:1000) with an overnight culture of pET32a-PPK2/*E. coli* BL21(DE3) and grown at 37 °C until the A_{600} reached 0.6. Protein expression was induced by addition of 0.5 mM isopropyl 1-thio-β-D-galactopyranoside (IPTG), and cultures were incubated at 25 °C for 6 h. After cooling to 4 °C, the cells were harvested by centrifugation and resuspended in buffer A [50 mM Tris-HCl (pH 6.8), 500 mM NaCl, 20 mM imidazole, 0.1% Triton X-100, and protease inhibitors (Complete, Roche Applied Science), 1 g of wet cell pellet/5 mL of buffer]. Cells were lysed by sonication (Sonics VibraCell, microtip, 30% power for 10 min, pulse on for 4.4 s, pulse off for 9.9 s with ice cooling) and then centrifuged (20 min at 30000*g* and 4 °C), and the supernatant was then filtered (Corning syringe filter, 0.2 μm) and directly loaded onto a 5 mL nickel-charged His-Trap chelating column (GE Life Sciences). The 5 mL column was washed with 25 mL of buffer A before the protein was eluted with a stepwise gradient over 100 mL versus buffer B [25 mM Tris-HCl (pH 6.8), 500 mM NaCl, and 550 mM imidazole]. The purest fractions [determined by sodium dodecyl sulfate−polyacrylamide gel electrophoresis (SDS−PAGE)] were combined and then frozen at −80 °C with 20% glycerol for long-term storage. Removal of the N-terminal tag was performed by thrombin cleavage according to the manufacturer's instructions (Novagen). In a reaction volume of 50 μL, 10 μg of PPK2 was incubated with 1 μL of 1:200 diluted thrombin for 3 h at room temperature. The extent of cleavage was analyzed by SDS−PAGE. The *V. cholerae* and *L. hongkongensis* PPK2 proteins were analogously expressed and purified, with the substitution of kanamycin for ampicillin (50 μg/mL).

Gel Filtration Chromatography. The molecular mass of recombinant *M. tuberculosis* PPK2 was determined by size exclusion chromatography using a Superdex-200 column (GE Life Sciences). The salt and imidazole were removed from the purified protein by dialysis against buffer C [50 mM sodium phosphate (pH 8.0), 200 mM NaCl, and 0.5 mM EDTA] before it was applied to the column equilibrated with the same buffer. The calibration was conducted using a gel filtration HMW calibration kit (GE Life Sciences) containing the proteins ovalbumin (43 kDa), aldolase (158 kDa), ferritin (440 kDa), and thyroglobulin (669 kDa). The void volume was determined with blue dextran 2000 (~2000 kDa).

Anion Exchange Chromatography. The reactivity of recombinant *M. tuberculosis* PPK2 with respect to polyP was characterized by anion exchange chromatography using a 1 mL Resource Q prepacked high-performance anion exchange column (GE

Life Sciences). The PPK2 reaction mixture containing 5 μg of PPK2 in 50 mM Tris-HCl (pH 8.0), a 2 mM AMP/ADP/ATP mixture, 5 mM $MnCl_2$, and 4 mg of $polyP_{65}$ in a final volume of 1.3 mL was incubated for 0−4 h at 25 °C. After 0, 2, and 4 h, 300 μL of each reaction mixture was injected into the anion exchange column, which was equilibrated with 10 column volumes of buffer [20 mM Tris-HCl (pH 8.5)]. The bound molecules were eluted with a 20 column volume stepwise salt concentration gradient [20 mM Tris-HCl (pH 8.5) and 0 to 1 M NaCl] at a flow rate of 1.5 mL/min. The eluted nucleotides were detected by UV absorption at 254 nm. The elution profile was analyzed using Data Analysis Software for VISION Workstation (Applied Biosystems).

Assays of PPK2. Activities of recombinant PPK2 were assayed spectrophotometrically using a previously described modified enzyme-coupled assay.[34,35] The nucleoside diphosphate kinase activity of recombinant PPK2 was measured in a reaction mixture (100 μL) containing 50 mM Tris-HCl (pH 8.5), 30 mM $MgCl_2$, 2 mM ADP (Sigma), 50 μg of $polyP_{65}$ (Sigma), 1 mM glucose, 1 mM NADP, 1 unit of hexokinase (Sigma), 1 unit of glucose-6-phosphate dehydrogenase (Sigma), and 1 μg of PPK2. The activity of the enzyme was quantified by NADPH formation using the A_{340} and compared with a standard ATP calibration curve. Kinetic parameters were determined by nonlinear curve fitting using Origin (Microcal Software). For optimization, temperatures from 25 to 45 °C for preincubation, $MnCl_2$ and $MgCl_2$ concentrations from 0 to 50 mM, and a pH range from 6.5 to 10.0 were used. ADP concentrations were varied up to 5 mM and $polyP_{65}$ concentrations up to 50 μM. For the PPK2 inhibition assay, the reaction mixture contained 50 mM Tris-HCl (pH 8.5), 30 mM $MgCl_2$, 2 mM ADP (Sigma), 100 mM KCl, 1 mM glucose, 1 mM NADP, 1 unit of hexokinase (Sigma), 1 unit of glucose-6-phosphate dehydrogenase (Sigma), 0−5 μM aptamer, and 1 μg of PPK2. The assay was started by the addition of $polyP_{65}$. The polyP synthesizing activity of PPK2 was measured with pyruvate kinase and lactate dehydrogenase. The reaction mixture contained 50 mM Tris-HCl (pH 8.5), 1 mM $MnCl_2$, 1 mM ATP (Sigma), 50 μg of $polyP_{65}$ (Sigma), 1 unit of pyruvate kinase (Sigma), 1 unit of lactate dehydrogenase (Sigma), 700 μM NADH (Sigma), 2 mM phosphoenolpyruvate (Sigma), and 10 μg of PPK2. The absorbance change due to the oxidation of NADH was measured at A_{340}.

***In Vitro* Aptamer Selection.** The selection of recombinant *M. tuberculosis* PPK2 aptamers relied on magnetic separation with the enzyme that was immobilized on the Ni-NTA magnetic beads (Qiagen) described previously.[36] The random single-stranded DNA library was chemically synthesized and purified by HPLC. The library was composed of 35 random nucleotides that were flanked by sequences suitable for amplification [5′-CCGTAATACGACTCACTATAGGGGAGCTCGGTAC-CGAATTC-(N35)-AAGCTTTGCAGAGAGGATCCTT-3′ (Molecular Informatrix Laboratory, Hong Kong, China)]. Primers that annealed to the 5′ and 3′ sequences flanking the degenerate region of the library used during the selection and cloning were SelexF (5′-CCGTAATACGACTCACTA-TAGGGGAGCTCGGTACCGAATTC-3′) and SelexR (5′-AAGGATCCTCTCTGCAAAGCTT-3′) in nonbiotinylated and 5′-biotinylated forms, respectively (HPLC-purified, Molecular Informatrix Laboratory). Iterative rounds of aptamer selection and amplification during the SELEX process were modified from the previous protocol.[36−38] Twenty rounds of selection were performed. The presence of G-quadruplex structure in aptamers was predicted by the quadruplex-forming G-rich sequence (QGRS) mapper.[39] Multiple-aptamer sequence alignments were performed with ClustalW2.[40]

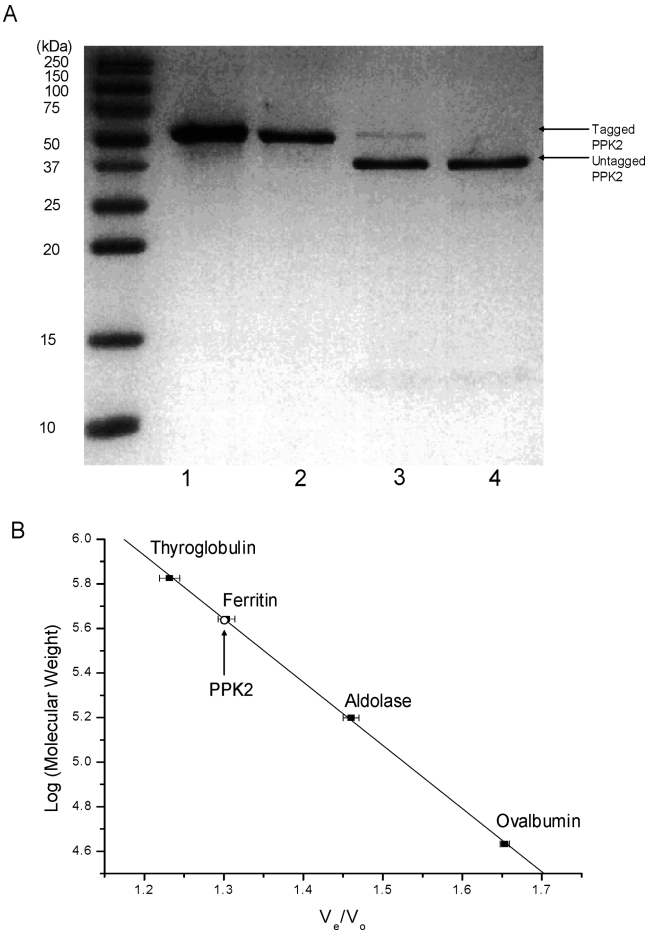

Figure 1. Purification and mass determination of *M. tuberculosis* PPK2. (A) SDS−PAGE (12%) of recombinant *M. tuberculosis* PPK2: lane 1, purified PPK2; lane 2, dialyzed PPK2; lane 3, partially untagged PPK2 after thrombin treatment for 2 h; lane 4, untagged PPK2 after thrombin treatment for 3 h. (B) Molecular mass determination of *M. tuberculosis* PPK2 by size exclusion chromatography. The molecular mass was plotted vs the elution volume/void volume ratio (V_e/V_o). The void volume was determined using blue dextran 2000. The elution position of the purified PPK2 is indicated by an empty circle.

Circular Dichroism Spectroscopy. Oligonucleotides (10 μM) were resuspended in 20 mM sodium phosphate buffer (pH 7.5) that contained 100 mM KCl or 100 mM NaCl. Samples were heated at 90 °C for 5 min, followed by gradual cooling to room temperature. CD spectra were recorded on a JASCO J-810 spectropolarimeter at 310−220 nm, by using four scans at a rate of 50 nm/min, a 1 s response time, a 1 nm bandwidth, and a 1 mm path length. The scans of the buffer alone were subtracted from the average scans for each sample.

Aptamer−Enzyme Linked Binding Assay. The assay was modified from previous protocols for the assessment of aptamer−protein interactions.[36,37,41,42] Ni-NTA HisSorb strips (Qiagen) were coated with 500 ng of purified proteins in 200 μL of coating buffer [50 mM Tris-HCl (pH 8.5), 100 mM NaCl, and 100 mM KCl] for 1.5 h at room temperature. The wells were washed four times with coating buffer. Biotinylated oligodeoxynucleotides (PPK2 NG1, PPK2 G9, thrombin binding aptamer, and oligonucleotide

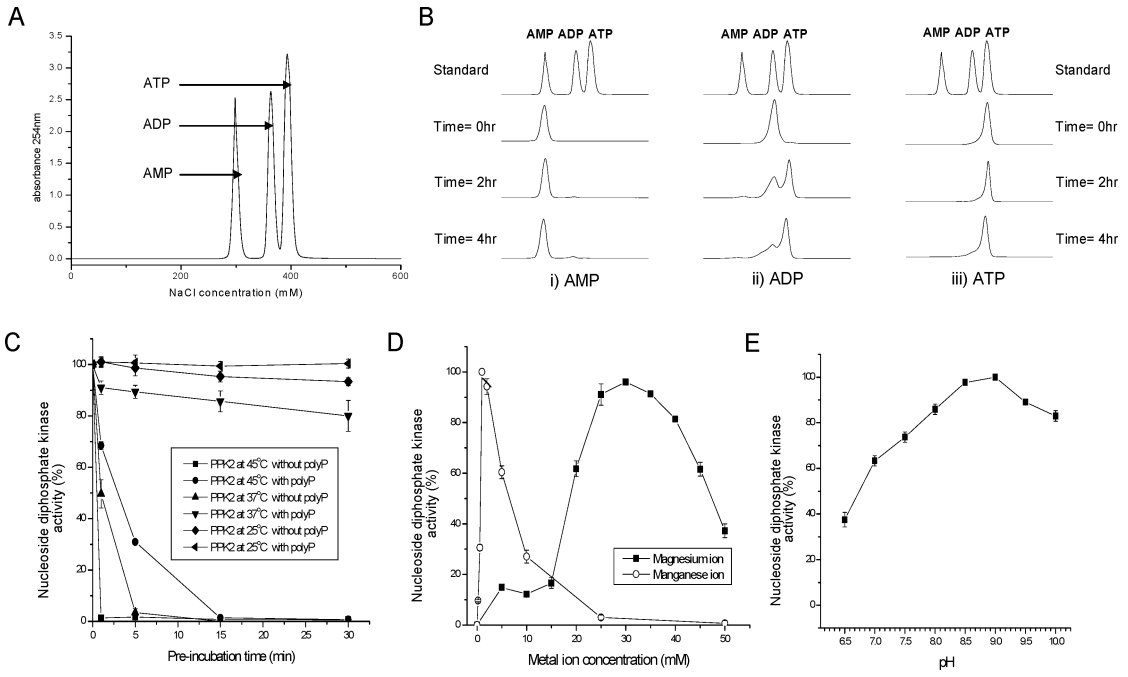

Figure 2. Biochemical characterization of *M. tuberculosis* PPK2. (A) Separation of adenosine nucleotide standards (AMP, ADP, and ATP) by anion exchange chromatography and detected by UV absorbance at 254 nm. (B) *M. tuberculosis* PPK2 was incubated with (i) AMP, (ii) ADP, or (iii) ATP, and phosphorylation or dephosphorylation of nucleotides in the presence of $polyP_{65}$ was observed. (C) *M. tuberculosis* PPK2 was preincubated with or without 50 μM $polyP_{65}$ at various temperature prior to the standard nucleoside diphosphate kinase activity assays. (D) Effects of magnesium and manganese ions on the nucleoside diphosphate kinase activities of the enzyme. (E) pH optima of the nucleoside diphosphate kinase reaction.

Table 1. Rate Constants for the PolyP Utilization and Synthesis Activities of *M. tuberculosis* PPK2

Reaction and Substrate	K_M (M)	k_{cat} (s^{-1})	k_{cat}/K_M (M^{-1} s^{-1})
polyP utilization reaction			
ADP	3.8×10^{-4}	41.9	1.1×10^{5}
$polyP_{65}$	6.3×10^{-6}	53.0	8.4×10^{6}
$polyP_{45}$	6.0×10^{-6}	50.0	8.3×10^{6}
polyP synthesis reaction			
ATP	3.3×10^{-4}	0.05	150
GTP	6.6×10^{-4}	0.08	121
$polyP_{65}$	5.4×10^{-6}	0.02	3704
$polyP_{45}$	5.0×10^{-6}	0.02	4000

35-mer random DNA sequence) were heated to 90 °C and then cooled quickly to 4 °C; 500 nM aptamers were incubated with protein in the HisSorb strips overnight at 4 °C with gentle shaking. Wells were washed six times with 200 μL of coating buffer for each wash for 10 min on a plate vortex. The streptavidin−horseradish peroxidase conjugate (Molecular Probes) was diluted 1:2000 in buffer, and 200 μL aliquots were applied to each well. Strips were incubated for 30 min at room temperature and washed again as described above. Then, 150 μL of Turbo-3,3′,5,5′-tetramethylbenzidine (TMB, Pierce) was added to each well and incubated for 20 min at room temperature in the dark. The reaction was quenched by addition of 150 μL of 1 M H_2SO_4, and the protein-bound aptamer−streptavidin complexes were quantified by determining the absorbance at 450 nm using SpectraMax Plus (Molecular Devices).

Isothermal Titration Calorimetry. The binding affinities and binding enthalpies of PPK2 G9 aptamers for *M. tuberculosis* PPK2 were measured by ITC (MicroCal VP-ITC, MicroCal Inc., Northampton, MA). In a typical ITC experiment, 20 μM *M. tuberculosis* PPK2 was loaded into the cell with 200 μM PPK2 G9 aptamers in the titrating syringe. Aptamers were weighed out as solids and dissolved into the buffer used for protein dialysis. The titration experiments were performed at 25 °C with an initial 0.2 μL injection, followed by thirty-one 1.2 μL injections. The time between injections was 150 s. The stirring speed during the titration was 900 rpm. Data were analyzed using MicroCal Origin by fitting to a single-site binding model.

RESULTS

Expression of Recombinant *M. tuberculosis* PPK2 and Biochemical Characterization. The *M. tuberculosis* genome encodes one homologue of the PPK2 protein (Rv3232c).[20] The *ppk2* (*PvdS*) gene was PCR amplified from *M. tuberculosis* H37Rv genomic DNA and cloned into pET32a(+). The N-terminally His-tagged protein was purified from the soluble fraction of induced cell lysates using nickel affinity chromatography (Figure 1A). Typical yields were 10 mg of purified protein/L of bacterial culture. Recombinant *M. tuberculosis* PPK2 was analyzed by gel filtration to show that *M. tuberculosis* PPK2 is an octamer (Figure 1B). PPK2 proteins from other bacteria have been reported to phosphorylate NDP to NTP with ATP synthesis at a rate 3-fold higher than the rate of GTP synthesis.[24] Using anion exchange chromatography, recombinant *M. tuberculosis* PPK2 directly demonstrated polyphosphate-dependent nucleoside diphosphate kinase (NDK) activity; i.e., it catalyzed the conversion of ADP to ATP with polyP acting as the phosphate donor (Figure 2A,B). No conversion of nucleotide was observed in the absence of polyP, suggesting that the reaction was

dx.doi.org/10.1021/bi2001455 |*Biochemistry* 2011, 50, 3261–3271

Aptamer clone	Core region of the aptamer sequences (5' to 3')	No. of nucleotide	Identical sequences
Group A: Non G-quadruplex aptamers			
	Conserved motif		
PPK2 NG1	---ATGTCCCCACCCTGT---TCAACCACTTGGCTACCGTTA	36	3
PPK2 NG2	--ACTATTCCCCCCCTGTATTTTCACCACTTGGGTTA-----	34	1
PPK2 NG3	---CGCTTACCCCCCTTATCTTCCACCACTTGGCCA------	32	1
PPK2 NG4	-GCCACCTCCCTACTTACCGTTCCACCACTTGGTC-------	33	2
PPK2 NG5	AGTTGTCTAGCCCCACACCATTTCACCACTTGGCCA------	35	3
PPK2 NG6	--ACAGTTGCCCCCTC--CATTTCACCTCTTGGTCGGTTA--	35	1
PPK2 NG7	------GTACCATCTT--CATTTCACCACTCGGTTTATCA--	30	2
PPK2 NG8	----ACAGTTGCCCCCTCCATTTCACCTCTTGGTCGGTTA--	35	1
Group B: G-quadruplex aptamers			
PPK2 G9	----AACACATAGG-TTTGGTTAGGTTGGTTGGTTGAATTA-	36	4
PPK2 G10	----AACACATAGG-TTTGGTTAGGTTGGTTGGTTGAATT--	35	4
PPK2 G11	-----AATCATAGG-GTTGGTTAGGTTGGTTGGTTGAATTA	35	3

Figure 3. Classification of in vitro-selected aptamer sequences against *M. tuberculosis* PPK2. Two groups of sequences were classified by the presence of G-quadruplex structures that was predicted by the QGRS mapper.

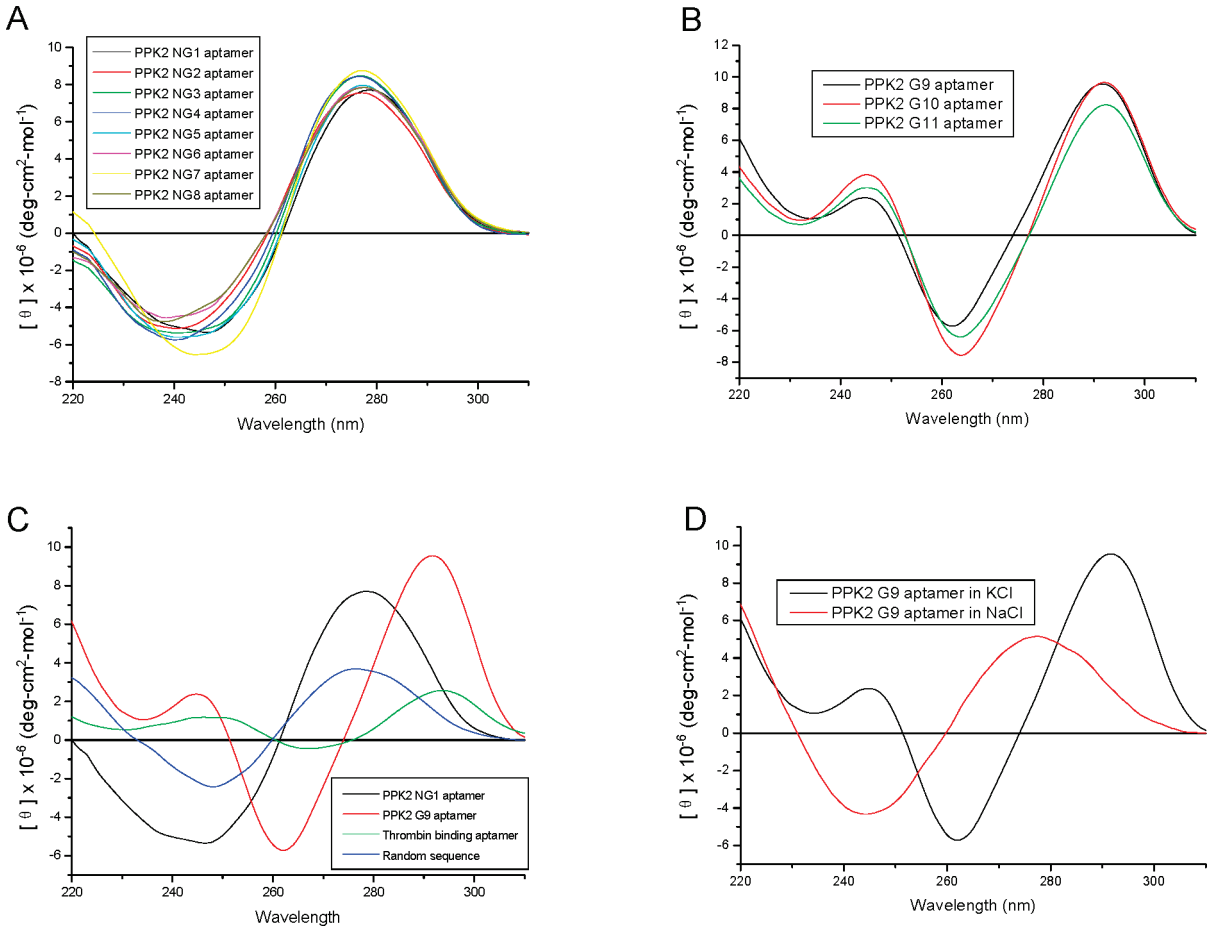

Figure 4. Structural analysis of selected DNA aptamers. CD spectrometry was performed for the PPK2 aptamers in (A) group A (non-G-quadruplex) and (B) group B (G-quadruplex) in 20 mM Na_3PO_4 (pH 7.5) and 100 mM KCl. (C) Comparison of CD spectra of the PPK2 NG1, the PPK2 G9 aptamer, thrombin binding aptamers, and random sequences in 20 mM Na_3PO_4 (pH 7.5) and 100 mM KCl. (D) CD spectra of the PPK2 G9 aptamer measured in the presence of either KCl or NaCl.

polyphosphate-dependent (Figure S1A of the Supporting Information). It has previously been reported that *E. coli* PPK can synthesize linear nucleoside tetraphosphates, via the transfer of a pyrophosphate group to the β-phosphate of nucleoside diphosphates.[43] Here, as we observed no formation of adenosine tetraphosphate in the chromatogram, we concluded that the *M. tuberculosis* PPK2 enzyme possessed no such activities. Additionally, the N-terminal His tag of the recombinant PPK2 had no

dx.doi.org/10.1021/bi2001455 |*Biochemistry* 2011, 50, 3261–3271

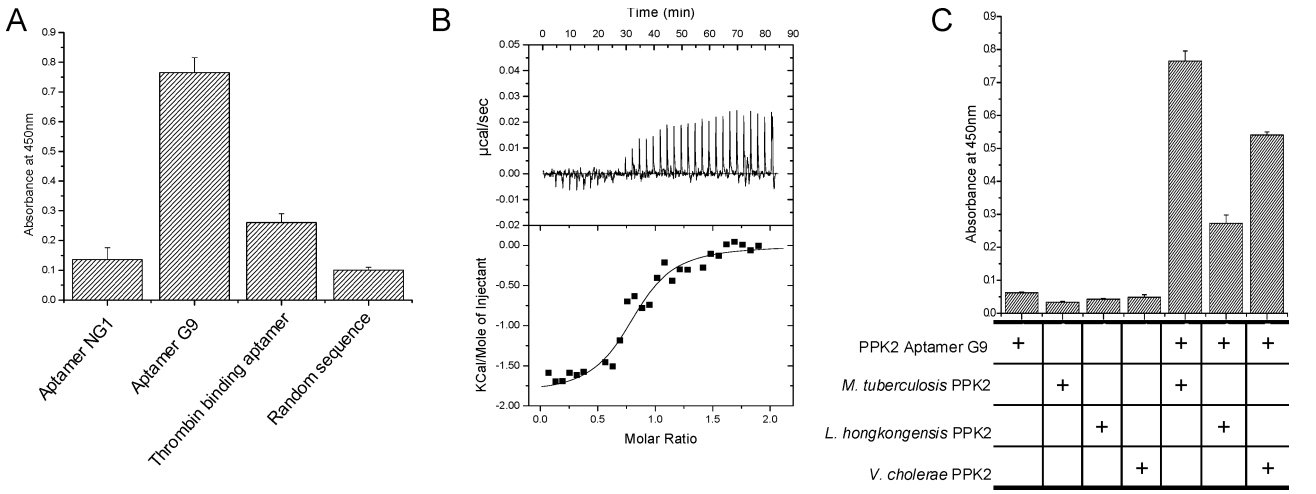

Figure 5. Binding of selected DNA aptamers. (A) Biotin-labeled aptamers and 35-mer random sequence (500 nM) were titrated with purified *M. tuberculosis* PPK2 immobilized on Ni-NTA HisSorb Strips. Their relative binding strength was measured by the absorbance at 450 nm. (B) Isothermal titration calorimetry analysis of the PPK2 G9 aptamer and *M. tuberculosis* PPK2 interaction. The top panel shows raw calorimetric data for serial injections of PPK2 G9 aptamers into *M. tuberculosis* PPK2. The bottom panel shows the binding isotherms resulting from integration of raw calorimetric data. (C) Relative binding of 500 nM PPK2 G9 aptamer to *M. tuberculosis* PPK2, *L. hongkongensis* PPK2, and *V. cholerae* PPK2.

effect on the protein's activities (Figure S1B of the Supporting Information).

The kinetics of recombinant *M. tuberculosis* PPK2 were quantitatively measured using enzyme-coupled assays. At low concentrations of nucleotides and polyP, the enzyme reaction followed simple single-site Michaelis−Menten behavior with the values of K_M, k_{cat}, and k_{cat}/K_M listed in Table 1. *M. tuberculosis* PPK2 exhibited comparable catalytic efficiencies (k_{cat}/K_M) for both polyP utilization and synthesis, but the polyP utilization reaction was 838 times faster. The enzyme was unable to use tri-polyP (P_3) or penta-polyP (P_5) as phosphate donors but exhibited similar catalytic activities with either $polyP_{45}$ or $polyP_{65}$. To investigate whether polyP stabilized PPK2, we preincubated recombinant *M. tuberculosis* PPK2 with or without polyP at 25, 37, and 45 °C prior to the activity assay (Figure 2C). In the absence of polyP, *M. tuberculosis* PPK2 exhibited low stability toward high temperatures in that the enzyme lost almost 100% of its activities after being preheated for 5 min at 37 and 45 °C. In contrast, in the presence of polyP, the enzyme activities remained at 90 and 30% after 5 min at 37 and 45 °C, respectively, suggesting that polyP stabilized the PPK2 protein structure. *M. tuberculosis* PPK2 can use either magnesium(II) or manganese-(II) for reaction. The optimal concentrations of magnesium(II) and manganese(II) were 30 and 1 mM, respectively, and the maximal activity of both ions was similar for the nucleoside diphosphate kinase activity (Figure 2D). Other metal ions such as iron(II), zinc(II), and copper(II) could not be used by the enzyme. *M. tuberculosis* PPK2 was active across a broad range of pH values, with optimal activity at pH ∼9 (Figure 2E). These results validated that *M. tuberculosis* PPK2 is a polyphosphate-dependent nucleoside diphosphate kinase.

Selection and Classification of DNA Aptamers against Recombinant *M. tuberculosis* PPK2. In an effort to develop inhibitors of recombinant *M. tuberculosis* PPK2, we screened for high-affinity DNA aptamers from a DNA random sequence pool. The starting library contained a random region of 35 nucleotides with an estimated complexity of 10^{21} unique sequences. As the *M. tuberculosis* PPK2 was overexpressed with a hexahistidine tag, we immobilized the protein on Ni-NTA magnetic beads and screened for binding aptamers from the pool. Twenty cycles of selection and amplification were performed. In total, 11 different sequences that were divided into two groups on the basis of their primary sequences and G-quadruplex structure prediction using the QGRS mapper [http://bioinformatics.ramapo.edu/QGRS (Figure 3)] and experimentally by circular dichroism (Figure 4A, B) were identified.[39] In group A (n = 8; NG1−NG8), high levels of sequence homology were observed, with a conserved motif present in all clones at approximately the same location in the random region [5′-TT(T/A)(C/A)ACC(A/T)CT(T/C)GG-3′] (Figure 3). In their CD spectra, all exhibited characteristics of a random sequence, typified by having positive peaks at 280 nm in their CD spectra (Figure 4A). In group B (n = 3; G9−G11), there was a repeat pattern of $(GGTTN)_n$ (where N is a deoxynucleotide and n is the number of repeats) (Figure 3). This stretch of nucleotides may be folded into an unusual guanosine quadruplex structure based on the guanine quartet, which should contribute substantial stability to the overall structure.[44] Their CD spectra were typified by a positive maximal peak near 295 nm, which indicates the presence of G-quadruplex structure. The 295 nm peak is analogous to that obtained for the thrombin binding aptamer (TBA) that contains antiparallel G-quadruplex structure revealed by X-ray crystallography and NMR (Figure 4C).[45] Additionally, the PPK2 G9 aptamer formed a G-quadruplex structure in buffer containing 100 mM potassium ions, but not in one that contained 100 mM sodium ions, which is consistent with previous reports that potassium-bound G-quadruplex structures are favored (Figure 4D).[46]

Binding of Selected Aptamers to PPK2. To take an initial measurement of the relative binding affinities of the aptamers for MTB PPK2, we employed an enzyme-linked assay in which His-tagged MTB PPK2 was immobilized on a plate and then biotinylated aptamers were added. Their relative binding affinities were quantified by an enzyme-linked immunoassay. We observed that only the G9 aptamer bound tightly to MTB PPK2, while the NG1 aptamer did not bind to the protein, similar to the thrombin binding aptamer and random sequence controls

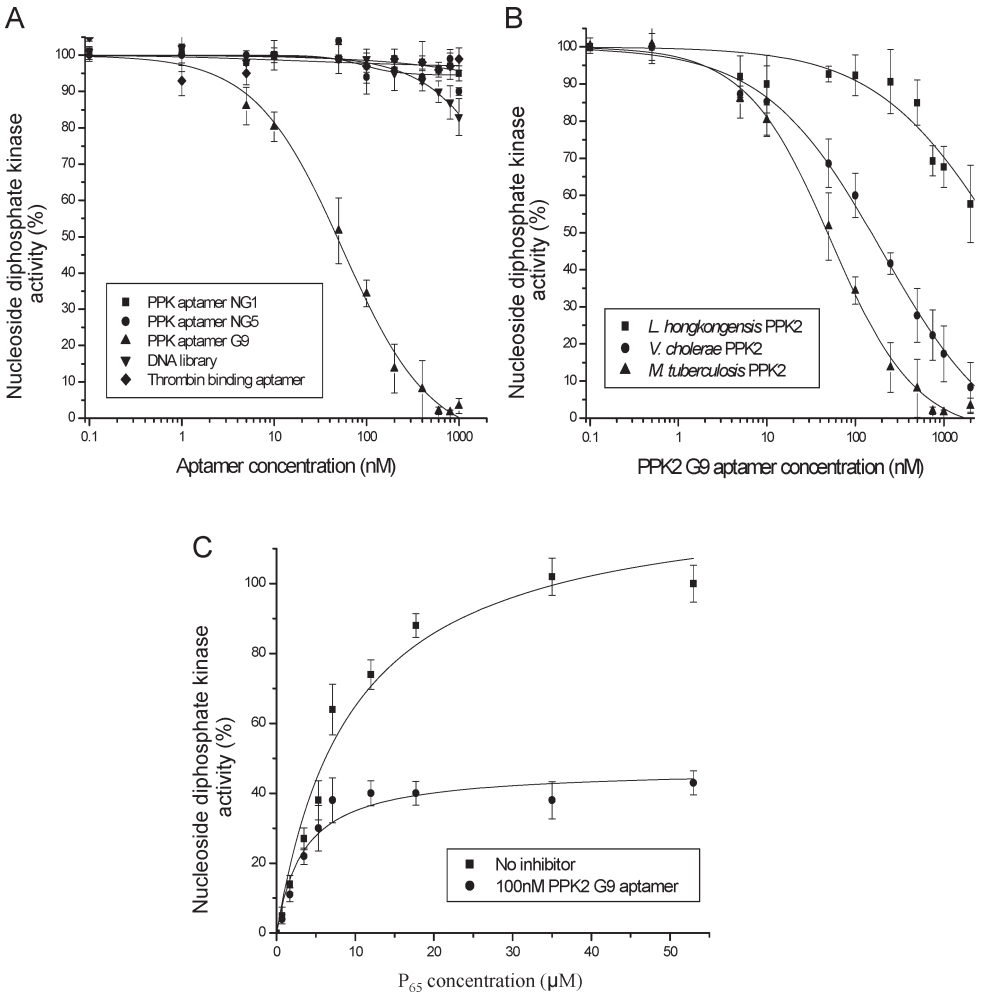

Figure 6. Inhibition of selected *M. tuberculosis* PPK2 aptamers. (A) Inhibition of *M. tuberculosis* PPK2 polyP-dependent nucleoside diphosphate kinase activity in the presence of various aptamers, the starting DNA library pool, and thrombin binding aptamers (TBA). (B) Inhibition of *M. tuberculosis*, *L. hongkongensis*, and *V. cholerae* PPK2 nucleoside diphosphate kinase activities by the PPK2 G9 aptamer. (C) Plot of the degree of inhibition of the PPK2 G9 aptamer vs the nucleoside diphosphate kinase activity of *M. tuberculosis* PPK2 measured at varying $polyP_{65}$ concentrations in the presence or absence of 100 nM PPK2 G9 aptamer.

(Figure 5A). Additionally, we employed isothermal titration calorimetry to quantitatively corroborate the interaction between MTB PPK2 and G9 aptamers. Our result showed that ~0.82 molecule of the G9 aptamer bound per monomeric PPK2 molecule (Figure 5B). The PPK2 G9 aptamer bound to PPK2 with a K_D of 870 ± 220 nM. The change in the free energy of binding (ΔG) was −8.25 ± 0.18 kcal/mol. The values of ΔH and ΔS reveal that the binding process is primarily driven by entropy with an enthalpy of binding (ΔH) at 25 °C of −1.85 ± 0.10 kcal/mol and an entropy of binding (ΔS) of 21.48 ± 0.94 cal mol^{-1} K^{-1}. The large entropic component of ΔG of binding may imply the release of ions or water molecules from the protein surface.

To investigate whether the G9 aptamer could also bind to PPK2 proteins from other species, we consequently cloned, expressed, and purified the PPK2 protein homologues from the β-proteobacterium *L. hongkongensis* and the γ-proteobacterium *V. cholerae* using an analogous approach. The PPK2 proteins from *L. hongkongensis* (LHK_00958) and *V. cholerae* (VC0728) are 54 and 64% identical in amino acid sequence to *M. tuberculosis* PPK2, respectively (Figure S2 of the Supporting Information). Analogous aptamer binding assays were separately performed with these PPK2 homologues (500 nM biotin-labeled aptamer added to 5.5 pmol of LHK or VC PPK2 protein immobilized on a Ni-NTA solid support) (Figure 5C). The PPK2 G9 aptamer exhibited different binding affinities for the two other PPK2 homologues, but both were significantly lower than the binding affinity for *M. tuberculosis* PPK2.

Aptamer-Mediated Inhibition of PPK2. Building on this foundation, we investigated whether representative aptamers inhibited the biochemical activities of the recombinant *M. tuberculosis* PPK2 protein. We employed an enzyme-coupled nucleoside diphosphate kinase assay to quantify any inhibitory activities. Potential inhibitors of the NDK reaction would be expected to reduce the amounts of ATP released, reflected in a proportional decrease in the level of NADPH formation measured at A_{340}. Controls using the starting DNA library pool and the authentic G-quadruplex thrombin binding aptamer were conducted to ensure the nucleic acids did not affect the enzyme's function in a nonspecific manner. *M. tuberculosis* PPK2 was titrated with an increasing concentration of the aptamer oligonucleotides. Our results showed differential inhibitory activities of the selected aptamers (Figure 6A). The DNA library pool and

dx.doi.org/10.1021/bi2001455 |*Biochemistry* 2011, 50, 3261–3271

group A (non-G-quadruplex) aptamers PPK2 NG1 and PPK2 NG5 inhibited the NDK activity of the MTB PPK2 protein to a negligible extent. Conversely, the G-quadruplex PPK2 G9 aptamer strongly inhibited the *M. tuberculosis* PPK2 protein with an IC_{50} value of 39.3 ± 10 nM. Additionally, the G-quadruplex aptamers inhibited *M. tuberculosis* PPK2 in the presence of 100 mM potassium ions but did not exhibit significant inhibitory activities when these were substituted with an equivalent concentration of sodium ions. Interestingly, the "authentic" G-quadruplex-containing thrombin binding aptamers did not inhibit the enzyme strongly, although they did have similar secondary structures, suggesting that the aptamer-mediated inhibition was sequence specific. The finding that the aptamer-mediated inhibition of the PPK2 NDK activity was dependent upon the presence of potassium ions appears to be linked to the results from the circular dichroism analysis of the aptamer structure and folding. This suggests that the potassium-bound G-quadruplex structures are intimately involved in PPK2 binding. As the PPK2 G9 aptamer bound to heterologous PPK2 proteins, we also investigated whether it acted as a more "general" PPK2 protein inhibitor. LHK and VC PPK2 proteins had activities analogous to that of MTB PPK2, and hence, comparative assays could be performed. In Figure 6B, the PPK2 G9 aptamer inhibited the NDK activities of both the LHK and VC PPK2 proteins, albeit more weakly than *M. tuberculosis* PPK2, with IC_{50} values of >1 μM and 105 ± 5 nM, respectively.

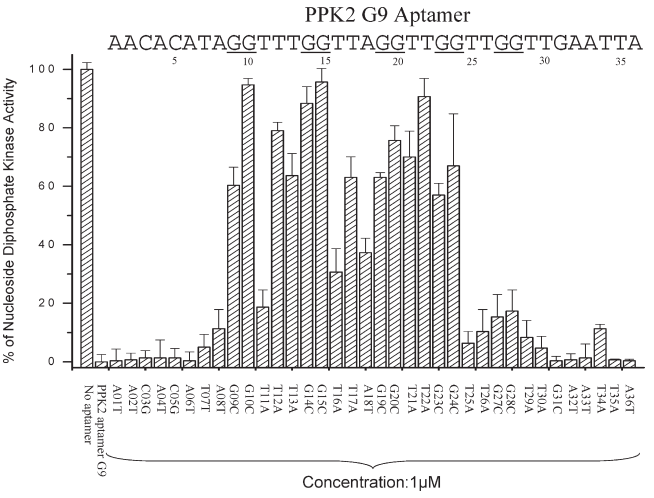

Figure 7. Mutational mechanistic analysis. The PPK2 G9 aptamer was mutated at every individual base position and then assayed for its ability to inhibit *M. tuberculosis* PPK2 nucleoside diphosphate kinase activity.

Determining the Mechanism of Inhibition. The X-ray crystal structures of the *Pseudomonas aeruginosa* (PA3455) and *Sinorhizobium meliloti* (SMc02148) PPK2 proteins were recently determined. These revealed a large positive charge surface distribution near the conserved Walker A (P-loop) and Walker B motifs, putatively involved in polyphosphate binding.[24] *M. tuberculosis* PPK2 has a secondary structure similar to the structures of these proteins based on the amino acid similarity (Figure S2 of the Supporting Information). Polyphosphates and aptamers are negative charge-carrying species that may competitively bind to the same positive surface patch of PPK2. Therefore, we tested the inhibition of NDK activity by the PPK2 G9 aptamer and checked the competition with respect to polyP. In Figure 6C, the reaction mixture was titrated with an increasing amount of polyP with or without aptamers. The result showed that aptamers caused significant reductions in the maximal effective rate of catalysis, V_{max} (from 110 ± 8 to 46.9 ± 3%), with small changes in K_M. In addition, the aptamers could bind to the free PPK2 in the binding assay (Figure 5), indicating that PPK2 G9 aptamer was acting as a noncompetitive inhibitor of the NDK activity of PPK2. This also suggests that the aptamer inhibits by binding at a site distinct from the active site where the substrates bind.

In addition, we mutated every base in aptamer G9 to pinpoint which nucleobases were critical to PPK2 inhibition (Figure 7). In the presence of 1 μM parent aptamer G9, PPK2 was inhibited almost 100% (Figure 7). When bases in aptamer G9 were individually mutated (A → T, T → A, G → C, and C → G), differing effects on inhibition were observed. Nucleobases near the 5′ end (positions 1−8) and 3′ end (positions 25−36) did not appear to play an important role in enzyme inhibition, with mutants having an effect similar to that of parent aptamer G9. However, nucleobases between G9 and G24 significantly reduced its inhibitory effect, particularly when guanine was changed to cytosine. The data support the possibility that these

Aptamer Clones	Aptamer Sequences (5' to 3')	IC_{50} (nM)
	1 5 10 15 20 25 30 35	
PPK2 G9	AACACATAGGTTTGGTTAGGTTGGTTGGTTGAATTA	39.3±10
PPK2 G9 m1	AACACATAGGTTTGGTTAGGTTGGTTGGTTG	50.3±8
PPK2 G9 m2	TAGGTTTGGTTAGGTTGGTTGGTTGAATTA	55.2±4
PPK2 G9 m3	TAGGTTTGGTTAGGTTGGTTGGTTG	58.4±9
PPK2 G9 m4	AGGTTTGGTTAGGTTGGTTGGTTG	250.0±14
PPK2 G9 m5	AGGTTTGGTTAGGTTGGTTGGTT	220.0±8
PPK2 G9 m6	GGTTTGGTTAGGTTGGTTGGTTG	450.5±10
PPK2 G9 m7	TTTGGTTAGGTTGGTTGGTTG	>1000
PPK2 G9 m8	GGTTAGGTTGGTTGGTTG	>1000
PPK2 G9 m9	TAGGTTTGGTTAGGTTGGTTGGTT	120.5±9
PPK2 G9 m10	TAGGTTTGGTTAGGTTGGTTGG	280.2±7
PPK2 G9 m11	TAGGTTTGGTTAGGTTGGTT	300.9±10
PPK2 G9 m12	TAGGTTTGGTTAGGTTGG	>1000
PPK2 G9 m13	GGTTTGGTTAGGTTGGTTGG	>1000
PPK2 G9 m14	GGTTTGGTTAGGTTGGTT	>1000

Figure 8. Truncation mechanistic analysis. The PPK2 G9 aptamer was truncated and assayed for its ability to inhibit *M. tuberculosis* PPK2 nucleoside diphosphate kinase activity.

guanine doublets (G9, G10; G14, G15; G19, G20; and G23, G24) may participate in G-quadruplex formation, which is necessary for PPK2 inhibition. As a second line of evidence, we truncated aptamer G9 to deduce the minimal length of functional aptamers (Figure 8). Interestingly, all truncated G9 aptamers adopt the G-quadruplex structure revealed by circular dichroism but differed in their IC_{50} values (Figure S3 of the Supporting Information). Aptamers that contained the first four guanine doublets retained significant inhibition (as indicated by clones m1−m6 and m9−m11), yet when the first guanine doublet was excluded, no inhibition was observed (as indicated by clones m7 and m8). However, additional bases are required to stabilize the G-quadruplex (as indicated by m11−m14). These data support the possibility that the guanine doublets (G9, G10; G14, G15; G19, G20; and G23, G24) are required but not sufficient for effective enzyme inhibition, and these doublets need further bases 5′ and 3′ for full stabilization of this G-quadruplex structure.

DISCUSSION

First identified by the late Arthur Kornberg fewer than 10 years ago,[20,22] PPK2 proteins are widely distributed throughput the microbial world, sharing high levels of sequence homology. Two general groups of PPK2 proteins have been structurally and biochemically characterized, which have one or two fused PPK2 domains.[24] *M. tuberculosis* PPK2 has one PPK2 domain similar to *P. aeruginosa* (PA0141) and *S. meliloti* (SMc02148) PPK2. Although belonging to the same group, *M. tuberculosis* PPK2 differs from its counterparts in certain ways. In terms of structure, native PA0141 and SMc02148 PPK2s are tetramers, which is illustrated by gel filtration and X-ray crystallography, while *M. tuberculosis* PPK2 is an octamer, possibly indicative of a different mode of catalysis. In addition, polyP synthesis was observed in *P. aeruginosa* PPK2 (although the rate was 75-fold lower than that of the polyP utilization reaction) but was almost undetectable in *M. tuberculosis* PPK2. However, both PPK2s function as nucleoside diphosphate kinases using polyP as a phosphate donor. Although the role of MTB PPK2 has been genetically characterized in mycobacteria, our biochemical characterization strengthens the view that PPK2 is a polyP-dependent nucleoside diphosphate kinase.

The *P. aeruginosa* PPK2 has been suggested to generate "energy-rich" nucleotides (e.g., GTP) used for alginate synthesis, an exopolysaccharide important in virulence for *P. aeruginosa*.[22] Consistent with this proposed function for PPK2, *M. tuberculosis* PPK2 is a polyP-dependent nucleoside diphosphate kinase that may also play a prominent role in making mycolic acids or other cell surface polysaccharides.[4,25] Because the polysaccharide components of the mycobacterial cell wall are absolutely essential for bacterial survival made during active cell growth, the mycobacteria must ensure a continuous and abundant supply of NTP to allow cell wall synthesis.[47] In addition, polyphosphate levels in mycobacteria have been shown to decrease during active cell growth and phosphate starvation and to increase during stationary periods for cell regeneration.[12,13,15,48] Using a *ppk2* knockout model, PPK2 was postulated to act as an energy bridge that balances the energy distribution stored in polyP within the cell.[4] Under circumstances when the ATP level is limiting, PPK2 may act to restore the ATP pool at the expense of polyP. This may be particularly important in the recovery of mycobacteria from dormancy to return to normal metabolic conditions. However, further detailed investigations are required to fully establish and delineate these putative roles played by the PPK2 protein in nucleotide homeostasis and cell wall synthesis.

Using SELEX methodology, we selected and modified DNA aptamers that bound tightly to recombinant *M. tuberculosis* PPK2 and inhibited its catalytic activities. Two groups of aptamers were identified: G-quadruplex and non-G-quadruplex. This work revealed differential inhibitory activities against *M. tuberculosis* PPK2 by two distinct aptamer groups that were isolated from the same library pool. The G-quadruplex PPK2 G9 aptamer was able to bind tightly to the protein and strongly inhibit its NDK activities. Conversely, the non-G-quadruplex aptamers (PPK2 NG1 and PPK2 NG5) exhibited poor inhibitory properties. There was clear specificity for the inhibitory properties of the G9 aptamer; VC PPK2 was inhibited to a lesser extent, and LHK PPK2 was inhibited at a far lower IC_{50}. Both the LHK and VC PPK2 proteins share a high degree of amino acid homology with *M. tuberculosis* PPK2 and have identical predicted secondary structures (Figure S2 of the Supporting Information). It is therefore difficult to identify likely structural or amino acid motif-based reasons for the differences in aptamer binding affinities.

Interestingly, the differential inhibitory activities of G-quadruplex versus non-G-quadruplex aptamers are opposite to those of our recently identified SARS coronavirus helicase aptamers, which also fell into two groups: those with or without G-quadruplexes. For the SARS-CoV helicase study, only the non-G-quadruplex aptamers were able to inhibit the helicase activities of the enzyme.[38] G-Quadruplexes are unusual DNA structures, shown to be present in a number of DNA aptamers. For example, the thrombin binding aptamer, which prevents blood clotting, has been extensively characterized as a G-quadruplex.[49] Nucleolin G-quadruplex-forming aptamer AS1411 is currently in clinical trial for cancer treatment.[50] The high-resolution three-dimensional structure of PPK2 revealed a large positive surface patch near the catalytic domain that is a potential binding site for our aptameric inhibitors,[24] although further work would be required to test this hypothesis. It is important to note that the SARS-CoV helicase aptameric inhibitors were competitive inhibitors, and this mechanistic difference may be important in the type of aptamers selected.

Therapeutic use of aptamers that target PPK2 in *M. tuberculosis* will require the development of suitable delivery systems or chemical conjugation strategies for enhancing mycobacterial uptake of exogenously added aptamers. Adding 5′ cell-penetrating peptides or 3′-poly-dG tails or alternatively "softening" the mycobacterial cell wall with antibiotics is an option that has been shown to successfully deliver therapeutic nucleic acid agents across the mycobacterial cell wall and inhibit the growth of mycobacteria.[32,33,51] These carriers show promise as tools for integrating together with inhibitory aptamers to target PPK2 within *M. tuberculosis*. Furthermore, we have previously shown that the stability of aptamers in serum could be significantly enhanced post-SELEX by capping 3′ termini with inverted thymidine.[37,38] Guanine nucleotides buried at the core of the G-quadruplex in the PPK2 aptamer may also contribute protection from nuclease attack. G-Quadruplex aptamer AS1411 was intact for 5 days in serum, while non-G-quadruplex random sequences lasted for only 1 h.[52] In summary, although enzymes involved in polyP metabolism have been suggested to be therapeutic targets for a long time,[7,20,26,53] this is the first study to demonstrate inhibition of a polyphosphate kinase that carries new mechanistic insight into G-quadruplex aptamer-mediated inhibition.

■ ASSOCIATED CONTENT

Supporting Information. Additional data. This material is available free of charge via the Internet at http://pubs.acs.org.

■ AUTHOR INFORMATION

Corresponding Author

*J.A.T.: Department of Biochemistry, The University of Hong Kong, 21 Sassoon Rd., Pokfulam, Hong Kong, China; telephone, (852) 28199472; fax, (852) 28551254; e-mail, jatanner@hkucc.hku.hk. R.M.W.: Oral Biosciences, Faculty of Dentistry, The University of Hong Kong, 34 Hospital Rd., Sai Ying Pun, Hong Kong, China; telephone, (852) 28590482; fax, (852) 25476257; e-mail, rmwatt@hku.hk.

Funding Sources

This work was supported by Hong Kong UGC GRF Grants HKU 776507M (to J.A.T.) and HKU 705007P (to R.M.W.) and by HKU Seed Funding Program for Basic Research Grants 200511159190 and 200411159146 (to J.A.T.).

■ ACKNOWLEDGMENT

We thank Prof. Wong Kam Bo (Department of Biochemistry, The Chinese University of Hong Kong, Hong Kong, China) for access to the circular dichroism spectropolarimeter.

■ ABBREVIATIONS

polyP, polyphosphate; ITC, isothermal titration calorimetry; PPK, polyphosphate kinase; MDR-TB, multidrug-resistant tuberculosis; SELEX, systematic evolution of ligands by exponential enrichment; NDK, nucleoside diphosphate kinase.

■ REFERENCES

(1) Zhang, Y., Post-Martens, K., and Denkin, S. (2006) New drug candidates and therapeutic targets for tuberculosis therapy. *Drug Discovery Today 11*, 21–27.

(2) Rao, N. N., and Kornberg, A. (1999) Inorganic polyphosphate regulates responses of *Escherichia coli* to nutritional stringencies, environmental stresses and survival in the stationary phase. *Prog. Mol. Subcell. Biol. 23*, 183–195.

(3) Rao, N. N., Gomez-Garcia, M. R., and Kornberg, A. (2009) Inorganic polyphosphate: Essential for growth and survival. *Annu. Rev. Biochem. 78*, 605–647.

(4) Sureka, K., Sanyal, S., Basu, J., and Kundu, M. (2009) Polyphosphate kinase 2: A modulator of nucleoside diphosphate kinase activity in mycobacteria. *Mol. Microbiol. 74*, 1187–1197.

(5) Jagannathan, V., Kaur, P., and Datta, S. (2010) Polyphosphate Kinase from *M. tuberculosis*: An Interconnect between the Genetic and Biochemical Role. *PLoS One 5*, e14336.

(6) Brown, M. R., and Kornberg, A. (2004) Inorganic polyphosphate in the origin and survival of species. *Proc. Natl. Acad. Sci. U.S.A. 101*, 16085–16087.

(7) Kornberg, A., Rao, N. N., and Ault-Riche, D. (1999) Inorganic polyphosphate: A molecule of many functions. *Annu. Rev. Biochem. 68*, 89–125.

(8) Shiba, T., Tsutsumi, K., Ishige, K., and Noguchi, T. (2000) Inorganic polyphosphate and polyphosphate kinase: Their novel biological functions and applications. *Biochemistry (Moscow, Russ. Fed.) 65*, 315–323.

(9) Kumble, K. D., and Kornberg, A. (1995) Inorganic polyphosphate in mammalian cells and tissues. *J. Biol. Chem. 270*, 5818–5822.

(10) Shiba, T., Tsutsumi, K., Yano, H., Ihara, Y., Kameda, A., Tanaka, K., Takahashi, H., Munekata, M., Rao, N. N., and Kornberg, A. (1997) Inorganic polyphosphate and the induction of rpoS expression. *Proc. Natl. Acad. Sci. U.S.A. 94*, 11210–11215.

(11) Smith, S. A., Mutch, N. J., Baskar, D., Rohloff, P., Docampo, R., and Morrissey, J. H. (2006) Polyphosphate modulates blood coagulation and fibrinolysis. *Proc. Natl. Acad. Sci. U.S.A. 103*, 903–908.

(12) Winder, F., and Denneny, J. M. (1954) Metaphosphate in mycobacterial metabolism. *Nature 174*, 353–354.

(13) Denneny, J. M., and Winder, F. G. (1956) Phosphorus metabolism of *Mycobacteria*: Determination of phosphorus compounds in some *Mycobacteria*. *J. Gen. Microbiol. 15*, 1–18.

(14) Varela, C., Mauriaca, C., Paradela, A., Albar, J. P., Jerez, C. A., and Chavez, F. P. (2010) New structural and functional defects in polyphosphate deficient bacteria: A cellular and proteomic study. *BMC Microbiol. 10*, 7.

(15) Winder, F. G., and Denneny, J. M. (1957) The metabolism of inorganic polyphosphate in mycobacteria. *J. Gen. Microbiol. 17*, 573–585.

(16) Guo, Y. L., Mayer, H., Vollmer, W., Dittrich, D., Sander, P., Schultz, A., and Schultz, J. E. (2009) Polyphosphates from *Mycobacterium bovis*: Potent inhibitors of class III adenylate cyclases. *FEBS J. 276*, 1094–1103.

(17) Sureka, K., Dey, S., Datta, P., Singh, A. K., Dasgupta, A., Rodrigue, S., Basu, J., and Kundu, M. (2007) Polyphosphate kinase is involved in stress-induced mprAB-sigE-rel signalling in mycobacteria. *Mol. Microbiol. 65*, 261–276.

(18) Manganelli, R. (2007) Polyphosphate and stress response in mycobacteria. *Mol. Microbiol. 65*, 258–260.

(19) Sureka, K., Ghosh, B., Dasgupta, A., Basu, J., Kundu, M., and Bose, I. (2008) Positive feedback and noise activate the stringent response regulator rel in mycobacteria. *PLoS One 3*, e1771.

(20) Zhang, H., Ishige, K., and Kornberg, A. (2002) A polyphosphate kinase (PPK2) widely conserved in bacteria. *Proc. Natl. Acad. Sci. U.S.A. 99*, 16678–16683.

(21) Lindner, S. N., Vidaurre, D., Willbold, S., Schoberth, S. M., and Wendisch, V. F. (2007) NCgl2620 encodes a class II polyphosphate kinase in *Corynebacterium glutamicum*. *Appl. Environ. Microbiol. 73*, 5026–5033.

(22) Ishige, K., Zhang, H., and Kornberg, A. (2002) Polyphosphate kinase (PPK2), a potent, polyphosphate-driven generator of GTP. *Proc. Natl. Acad. Sci. U.S.A. 99*, 16684–16688.

(23) Gangaiah, D., Liu, Z., Arcos, J., Kassem, I. I., Sanad, Y., Torrelles, J. B., and Rajashekara, G. (2010) Polyphosphate kinase 2: A novel determinant of stress responses and pathogenesis in *Campylobacter jejuni*. *PLoS One 5*, e12142.

(24) Nocek, B., Kochinyan, S., Proudfoot, M., Brown, G., Evdokimova, E., Osipiuk, J., Edwards, A. M., Savchenko, A., Joachimiak, A., and Yakunin, A. F. (2008) Polyphosphate-dependent synthesis of ATP and ADP by the family-2 polyphosphate kinases in bacteria. *Proc. Natl. Acad. Sci. U.S.A. 105*, 17730–17735.

(25) Kornberg, A. (2008) Abundant Microbial Inorganic Polyphosphate, Poly P Kinase Are Underappreciated. *Microbe 3*, 119–123.

(26) Brown, M. R., and Kornberg, A. (2008) The long and short of it: Polyphosphate, PPK and bacterial survival. *Trends Biochem. Sci. 33*, 284–290.

(27) Tuerk, C., and Gold, L. (1990) Systematic evolution of ligands by exponential enrichment: RNA ligands to bacteriophage T4 DNA polymerase. *Science 249*, 505–510.

(28) Jayasena, S. D. (1999) Aptamers: An emerging class of molecules that rival antibodies in diagnostics. *Clin. Chem. 45*, 1628–1650.

(29) Ng, E. W., Shima, D. T., Calias, P., Cunningham, E. T., Jr., Guyer, D. R., and Adamis, A. P. (2006) Pegaptanib, a targeted anti-VEGF aptamer for ocular vascular disease. *Nat. Rev. Drug Discovery 5*, 123–132.

(30) Rimmele, M. (2003) Nucleic acid aptamers as tools and drugs: Recent developments. *ChemBioChem 4*, 963–971.

(31) Bunka, D. H., and Stockley, P. G. (2006) Aptamers come of age: At last. *Nat. Rev. Microbiol. 4*, 588–596.

(32) Harth, G., Horwitz, M. A., Tabatadze, D., and Zamecnik, P. C. (2002) Targeting the *Mycobacterium tuberculosis* 30/32-kDa mycolyl transferase complex as a therapeutic strategy against tuberculosis: Proof of principle by using antisense technology. *Proc. Natl. Acad. Sci. U.S.A. 99*, 15614–15619.

(33) Harth, G., Zamecnik, P. C., Tang, J. Y., Tabatadze, D., and Horwitz, M. A. (2000) Treatment of *Mycobacterium tuberculosis* with antisense oligonucleotides to glutamine synthetase mRNA inhibits glutamine synthetase activity, formation of the poly-L-glutamate/glutamine cell wall structure, and bacterial replication. *Proc. Natl. Acad. Sci. U.S.A. 97*, 418–423.

(34) Robinson, N. A., and Wood, H. G. (1986) Polyphosphate kinase from *Propionibacterium shermanii*. Demonstration that the synthesis and utilization of polyphosphate is by a processive mechanism. *J. Biol. Chem. 261*, 4481–4485.

(35) Robinson, N. A., Clark, J. E., and Wood, H. G. (1987) Polyphosphate kinase from *Propionibacterium shermanii*. Demonstration that polyphosphates are primers and determination of the size of the synthesized polyphosphate. *J. Biol. Chem. 262*, 5216–5222.

(36) Murphy, M. B., Fuller, S. T., Richardson, P. M., and Doyle, S. A. (2003) An improved method for the in vitro evolution of aptamers and applications in protein detection and purification. *Nucleic Acids Res. 31*, e110.

(37) Shum, K. T., Chan, C., Leung, C. M., and Tanner, J. A. (2011) Identification of a DNA aptamer that inhibits sclerostin's antagonistic effect on Wnt signalling. *Biochem. J. 434*, 493–501.

(38) Shum, K. T., and Tanner, J. A. (2008) Differential inhibitory activities and stabilisation of DNA aptamers against the SARS coronavirus helicase. *ChemBioChem 9*, 3037–3045.

(39) Kikin, O., D'Antonio, L., and Bagga, P. S. (2006) QGRS Mapper: A web-based server for predicting G-quadruplexes in nucleotide sequences. *Nucleic Acids Res. 34*, W676–W682.

(40) Larkin, M. A., Blackshields, G., Brown, N. P., Chenna, R., McGettigan, P. A., McWilliam, H., Valentin, F., Wallace, I. M., Wilm, A., Lopez, R., Thompson, J. D., Gibson, T. J., and Higgins, D. G. (2007) Clustal W and Clustal X version 2.0. *Bioinformatics 23*, 2947–2948.

(41) Stevenson, R., Baxter, H. C., Aitken, A., Brown, T., and Baxter, R. L. (2008) Binding of 14-3-3 proteins to a single stranded oligodeoxynucleotide aptamer. *Bioorg. Chem. 36*, 215–219.

(42) Choi, M. Y., Chan, C. C., Chan, D., Luk, K. D., Cheah, K. S., and Tanner, J. A. (2009) Biochemical consequences of sedlin mutations that cause spondyloepiphyseal dysplasia tarda. *Biochem. J. 423*, 233–242.

(43) Kuroda, A., and Kornberg, A. (1997) Polyphosphate kinase as a nucleoside diphosphate kinase in *Escherichia coli* and *Pseudomonas aeruginosa*. *Proc. Natl. Acad. Sci. U.S.A. 94*, 439–442.

(44) Huppert, J. L. (2008) Four-stranded nucleic acids: Structure, function and targeting of G-quadruplexes. *Chem. Soc. Rev. 37*, 1375–1384.

(45) Kelly, J. A., Feigon, J., and Yeates, T. O. (1996) Reconciliation of the X-ray and NMR structures of the thrombin-binding aptamer d(GGTTGGTGTGGTTGG). *J. Mol. Biol. 256*, 417–422.

(46) Shafer, R. H., and Smirnov, I. (2000) Biological aspects of DNA/RNA quadruplexes. *Biopolymers 56*, 209–227.

(47) Chakrabarty, A. M. (1998) Nucleoside diphosphate kinase: Role in bacterial growth, virulence, cell signalling and polysaccharide synthesis. *Mol. Microbiol. 28*, 875–882.

(48) Rifat, D., Bishai, W. R., and Karakousis, P. C. (2009) Phosphate depletion: A novel trigger for *Mycobacterium tuberculosis* persistence. *J. Infect. Dis. 200*, 1126–1135.

(49) Macaya, R. F., Schultze, P., Smith, F. W., Roe, J. A., and Feigon, J. (1993) Thrombin-binding DNA aptamer forms a unimolecular quadruplex structure in solution. *Proc. Natl. Acad. Sci. U.S.A. 90*, 3745–3749.

(50) Que-Gewirth, N. S., and Sullenger, B. A. (2007) Gene therapy progress and prospects: RNA aptamers. *Gene Ther. 14*, 283–291.

(51) Kulyte, A., Nekhotiaeva, N., Awasthi, S. K., and Good, L. (2005) Inhibition of *Mycobacterium smegmatis* gene expression and growth using antisense peptide nucleic acids. *J. Mol. Microbiol. Biotechnol. 9*, 101–109.

(52) Dapic, V., Bates, P. J., Trent, J. O., Rodger, A., Thomas, S. D., and Miller, D. M. (2002) Antiproliferative activity of G-quartet-forming oligonucleotides with backbone and sugar modifications. *Biochemistry 41*, 3676–3685.

(53) Rashid, M. H., Rumbaugh, K., Passador, L., Davies, D. G., Hamood, A. N., Iglewski, B. H., and Kornberg, A. (2000) Polyphosphate kinase is essential for biofilm development, quorum sensing, and virulence of *Pseudomonas aeruginosa*. *Proc. Natl. Acad. Sci. U.S.A. 97*, 9636–9641.